Density of states and spatially inhomogeneous conductance near the metal–insulator transition in $Pr_{0.68}Pb_{0.32}MnO_3$ single crystals

2008 J. Phys.: Condens. Matter 20 434231

(http://iopscience.iop.org/0953-8984/20/43/434231)

J. Phys.: Condens. Matter **20** (2008) 434231 (5pp) doi:10.1088/0953-8984/20/43/434231

Density of states and spatially inhomogeneous conductance near the metal–insulator transition in $Pr_{0.68}Pb_{0.32}MnO_3$ single crystals

S Wirth[1], Sahana Rößler[1], S Ernst[1], B Padmanabhan[2], H L Bhat[2], Suja Elizabeth[2] and F Steglich[1]

[1] Max Planck Institute for Chemical Physics of Solids, Nöthnitzer Straße 40, 01187 Dresden, Germany
[2] Department of Physics, Indian Institute of Science, Bangalore 560012, India

Received 7 July 2008
Published 9 October 2008
Online at stacks.iop.org/JPhysCM/20/434231

Abstract

Single crystals of $Pr_{0.68}Pb_{0.32}MnO_3$ have been investigated by scanning tunneling microscopy over a broad temperature range. In this material, a distinct separation of the ferromagnetic and the metal–insulator transition temperature, $T_C \approx 210$ K and $T_{MI} \approx 255$ K, respectively, was observed. Spectroscopic tunneling studies revealed that even on a local scale the system switches from predominantly metallic to insulating within a narrow temperature range around T_{MI}. Inhomogeneities of the zero-bias conductance with small patches of metallic clusters on a length scale of 2–3 nm, however, were only observed within the temperature range $T_C < T < T_{MI}$. The results give direct evidence for phase separation in the paramagnetic metallic state, but homogeneous ferromagnetic and insulating states.

Doped manganites in which some of the trivalent ions A^{3+} in the parent compound $AMnO_3$ are replaced by divalent ions B^{2+} to form $A_{1-x}B_xMnO_3$ have become very popular over the past 15 years since they not only show rich physics and a number of extraordinary effects but may also provide many opportunities for applications [1]. The origin of the vast number of phenomena stems, in many cases, from an interplay of lattice, charge, orbital and spin degrees of freedom which all take place at comparable energy scales [2]. At around 30% hole doping ($x = 0.3$) most of these compounds (such as $La_{0.7}Ca_{0.3}MnO_3$ and $La_{0.7}Ba_{0.3}MnO_3$) have a half-metallic ferromagnetic ground state due to strong Hund coupling and are subject to so-called Jahn–Teller (JT) distortion inflicted by the Mn^{3+} ions in the mixed-valence manganites [3]. At increased temperatures these materials exhibit a metal–insulator transition (MIT) at T_{MI} beyond which the electronic transport is dominated by polaronic hopping. For a certain doping x, this transition can be associated with a ferromagnetic transition temperature T_C. Near the MIT a large magnetoresistance (the so-called colossal magnetoresistance, CMR) can frequently be observed. It is the aforementioned similarity of the energy scales involved that makes these materials susceptible to separation into a metallic ferromagnetic phase and a insulating paramagnetic one, specifically close to the transition temperatures [4].

Phase separation (PS) in relation to the MIT has been discussed from both a theoretical and an experimental point of view. Monte Carlo simulation by Dagotto and co-workers (see, e.g., [5]), taking into account double exchange, JT interaction and the long-range Coulomb potential on two active e_g orbitals per Mn ion, pointed towards PS on a nanometer scale. Very recently, analytical calculations [6, 7] based on a Hamiltonian as similarly used to describe heavy fermion physics also favored PS. A number of early experiments including electron microscopy [8], scanning probe techniques such as magnetic force [9] and scanning tunneling microscopy/spectroscopy (STM/S) [10], as well as photoelectron spectroscopy [11], however, showed randomly shaped inhomogeneities on a scale of several hundred nanometers. In this context quenched disorder in the couplings resulting from the chemical doping was discussed [12].

It is well known that the nature of electronic transport is influenced by strain and microstructure of the specimen under investigation. A similar argument holds for PS as seen, for

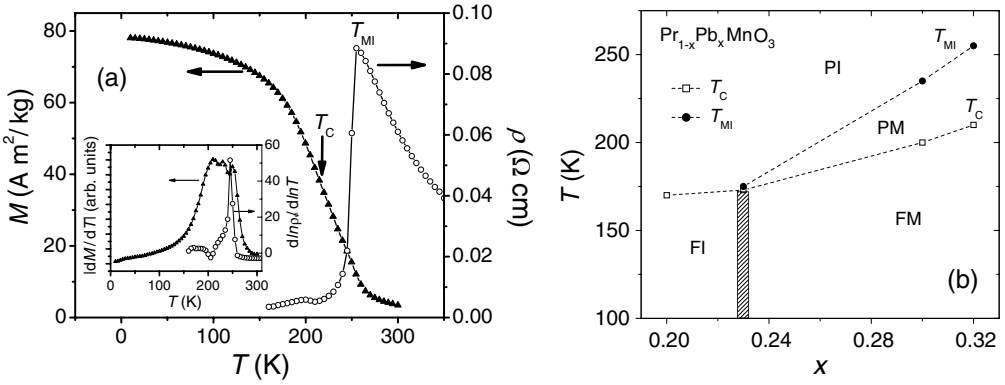

Figure 1. (a) Temperature dependence of the magnetization M (left scale) and of the zero-field resistivity ρ (right scale) of the $Pr_{0.68}Pb_{0.32}MnO_3$ single crystal. T_C and T_{MI} are indicated for the respective curves. Inset: the derivatives $|dM/dT|$ and $d\ln\rho/d\ln T$ allow for a comparison of the width of the two transitions. (b) Partial phase diagram of $Pr_{1-x}Pb_xMnO_3$ for $0.2 \leqslant x \leqslant 0.32$ illustrating the distinct values of T_C and T_{MI} for $x > 0.23$.

example, in noise measurements: two-level fluctuations of the resistance indicated switching of nanometer-scale clusters between two conductance states implying PS [13]. However, relaxing the strain by using a well-matching substrate for film deposition reduced the spectral noise density by four orders of magnitude [14], i.e. the PS was much less developed. Similar conclusions were reached in recent STS studies: in $La_{0.75}Ca_{0.25}MnO_3$ thin films PS was found to persist deep into the metallic regime only in case of A site disorder [15] and no PS could be observed for strain-relaxed $La_{0.7}Ca_{0.3}MnO_3$ on $NdGaO_3$ [16]. In order to minimize strain we concentrated our investigations on single crystals which also excluded any ambiguity that might stem from grain boundaries or grain misorientation in polycrystalline samples. It should also be mentioned that the tolerance factor t in our material is very close to unity, $t = 0.965$. This implies an intrinsically relaxed overall lattice structure. As a result, the normalized derivative of the resistivity, $d\ln\rho/d\ln T$, displays a very sharp peak (see inset to figure 1(a)) with a width of about 10 K. It was shown for manganite films deposited onto different substrate materials that this is indicative of a strain-relaxed material [17]. On the other hand, small local structural distortions due to the difference in ionic radii of Pr^{3+} and Pb^{2+} cannot be excluded.

In contrast to the MIT the magnetic transition is smeared over a broad temperature range (figure 1(a)). We therefore took the midpoint of the static M–T curve as $T_C \approx 210$ K. Such a definition is supported by a detailed scaling analysis on a sample from the same batch [18]. The analysis is similar to one used for Arrott plots but with critical exponents corresponding to an isotropic three-dimensional Heisenberg ferromagnet. Moreover, heat capacity measurements pointed towards a similar value of T_C [19]. Hence, T_C in our sample $Pr_{0.68}Pb_{0.32}MnO_3$ is distinctly lower than T_{MI}. This difference is observed for doping $x > 0.23$ [20] as see in the partial phase diagram figure 1(b). A possible explanation [21] is the formation of ferromagnetic clusters below T_{MI} and electronic conduction taking place by tunneling between these clusters through an insulating matrix. This interpretation is in accord with our observation of the material's magnetic susceptibility systematically deviating from a Curie–Weiss behavior for $T <$ 255 K. The formation of small (∼1.2 nm) localized magnetic clusters above T_C was also observed in doped $La_{2/3}Ca_{1/3}MnO_3$ and was put in context with the CMR properties [22].

STM is a highly surface sensitive technique and, hence, special attention has to be paid to surface preparation. Cubic manganites, in contrast to the layered ones [23], do not cleave. *In situ* sample growth, an elaborate way to circumvent this problem, can be applied for thin films [24] but not in case of single crystals. Therefore, the sample surface was scratched *ex situ* while immersed in alcohol and immediately loaded into our ultra-high vacuum system. STM was conducted using tungsten tips, 0.3 nA for the set point of the tunneling current I and a typical bias voltage $V = 0.8$ V, i.e. tunneling into the unoccupied density of states (DOS) of the sample. We conducted STS exclusively on surface areas that (i) showed atomically flat terraces with step heights corresponding to the unit cell height for the ⟨100⟩ surface of the pseudocubic perovskite crystal and (ii) exhibited the expected exponential dependence of I on the relative tip–sample distance z over at least two orders in magnitude of I and with a derived work function $\phi \geqslant 1$ eV. The latter ensures a good vacuum tunnel barrier. Tunneling spectra were obtained in 1 nm steps over an area of 50×50 nm^2. Figure 2(a) presents the I–V curves averaged over the resulting set of 2500 curves and figure 2(b) displays the simultaneously measured (via lock-in technique) derivative dI/dV, the latter being proportional to the sample's *local* DOS near the Fermi level. With $T_C \approx 210$ K and $T_{MI} \approx 255$ K, the temperatures 80, 234 and 260 K shown in figure 2 are representative of the three different regimes $T < T_C$, $T_C < T < T_{MI}$ and $T > T_{MI}$, respectively. The expected temperature evolution is obvious: at temperatures below T_{MI} a *finite* zero-bias conductance $G_0 = G(V = 0) = dI/dV|_{V=0}$ was observed, whereas at $T > T_{MI}$ we found $G_0 \approx 0$. This temperature dependence of G_0 is summarized in figure 4(a) (crosses). The sharp drop of G_0 at a temperature very close to the bulk T_{MI} suggests that our STS data are *not* dominated by surface effects.

So far, spatially averaged (over 2500 individual curves within a 50×50 nm^2 area) spectroscopy has been presented. To tackle the problem of PS, locally resolved spectroscopy

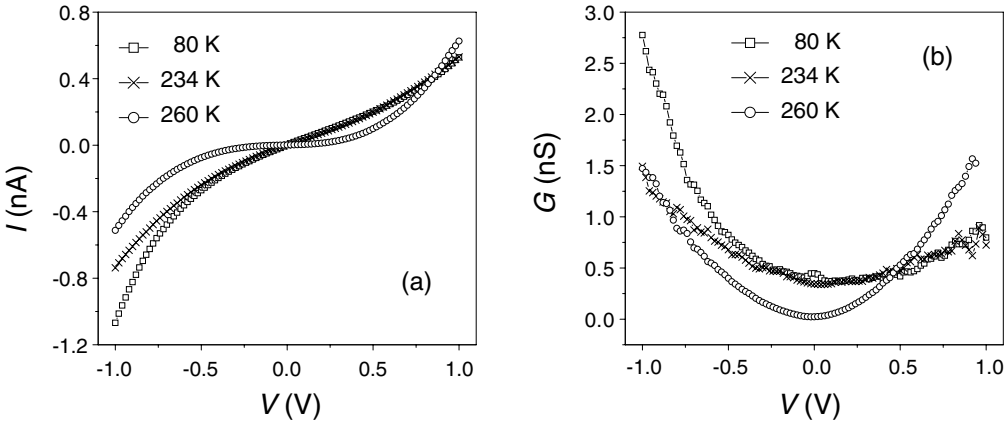

Figure 2. (a) Tunneling spectroscopy (I–V) curves and (b) simultaneously measured conductance ($G = \mathrm{d}I/\mathrm{d}V$) curves averaged over 2500 individual curves obtained over an area of 50 × 50 nm^2. The three temperatures are representative of the three different regimes: metallic behavior at $T = 80$ K $< T_C$, predominantly metallic for $T_C < T = 234$ K $< T_{MI}$ and insulating above T_{MI} with $G(V = 0) \approx 0$.

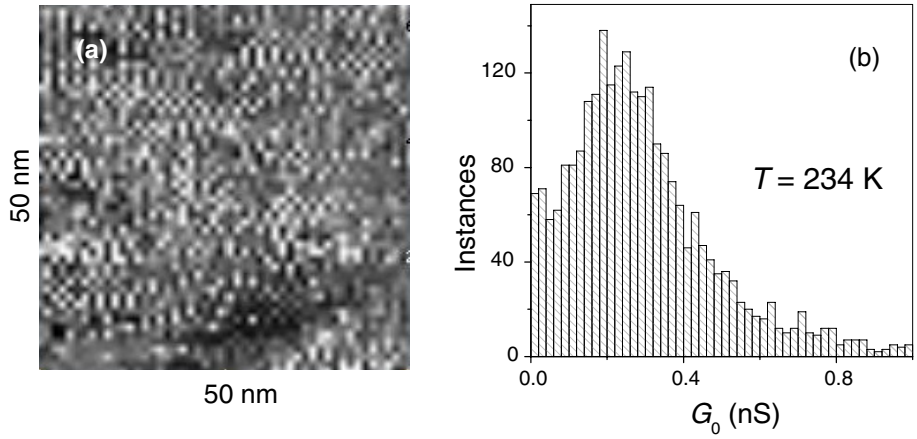

Figure 3. (a) STS conductance map over an area of 50 × 50 nm^2 at 234 K. The gray scale indicates the zero-bias conductance G_0 (black, $G_0 = 0$; white, $G_0 = 1.0$ nS). (b) The histogram shows how often a given value of G_0 was found within (a). The clearly inhomogeneous distribution indicates phase separation.

(cf figure 3(a)) is to be considered, with the metallic and insulating phases distinguished by their different conductances [25]. The first experiments reported in the literature [10] showed locally resolved conductance maps obtained at bias voltage $V = 3$ V (an order of magnitude larger than the semiconducting gap), and hence the system may *not* be in its ground state. Detailed local measurements of the zero-bias conductance on $La_{0.7}Sr_{0.3}MnO_3$ thin films at different temperatures were also reported [26]. However, a *single, temperature independent* threshold value for G_0 was applied to distinguish between the phases. Note that any repeatedly measured value (here G_0) will always show a certain distribution (with its width given by the experimental accuracy) which, along with a temperature dependence, may be interpreted as PS in such an analysis. Therefore, the whole distribution of G_0 values needs to be considered [27] as shown in figure 3(b). In this histogram, the number of occurrences of the G_0 values in the STS conductance map of figure 3(a) is presented. We emphasize the following two observations:

(i) The distribution of G_0 at $T = 234$ K is very broad. At high temperature ($T = 300$ K $> T_{MI}$) we find a G_0 distribution that can be well described by a Lorentzian with a maximum very close to $G_0 = 0$ and a full width at half-maximum (FWHM) of only 20 pS. At low temperature ($T = 30$ K) the maximum of the G_0 distribution was observed at about 0.37 nS with a FWHM of 30 pS. The latter two distributions are both more than an order of magnitude smaller in width compared with the one at $T = 234$ K. Such broadened distributions were found for all intermediate temperatures $T_C < T < T_{MI}$. The G_0 values of the main maximum of the distributions at different temperatures are given in figure 4(a), marked as the main histogram peak (open circles); they roughly follow the $G_0(T)$ values obtained from the averaged $\mathrm{d}I/\mathrm{d}V$ curves (crosses). The slight increase of G_0 just below T_{MI} is probably caused by the broad distribution of G_0.

(ii) At intermediate temperatures, the distribution cannot be described by a single distribution. Rather, there seems to be a broad distribution with a maximum at $G_0 \approx 0.24$ nS and another one with its maximum close to $G_0 = 0$. We propose that the former maximum corresponds to the metallic phase whereas the latter reflects the insulating

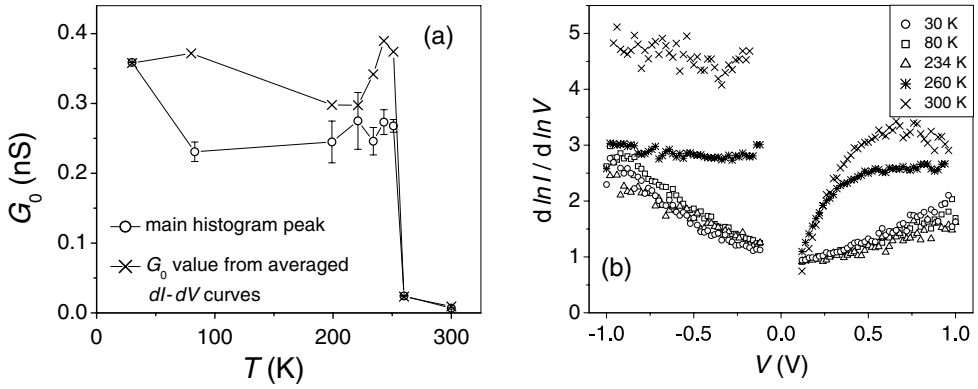

Figure 4. (a) Temperature dependence of G_0 obtained from averaged conductance curves at $V = 0$ ($\times$, cf figure 2(b)) and from the main peak in the conductance distribution ($\circ$, cf figure 3(b)). (b) Normalized conductance in dependence on V for selected temperatures. The drastic change of the sample's DOS near E_f when crossing T_{MI} is obvious.

one. The predominance of the former maximum is in agreement with the overall metallic behavior at $T < T_{\mathrm{MI}}$. The appearance of two maxima, however, is clear evidence of phase separation. Importantly, this PS is only observed for temperatures $T_{\mathrm{C}} < T < T_{\mathrm{MI}}$.

We note that the length scale of the observed spatial conductance inhomogeneities is 2–3 nm (cf figure 3(a)) in good agreement with theoretical predictions [5], but in contrast to earlier investigations [10]. Moreover, no hint of PS was observed for $T < T_{\mathrm{C}}$, in contrast to earlier reports of PS deep in the metallic regime. It appears plausible that the extent of PS diminishes as any strain in the sample is relaxed. However, it remains to be seen whether this finding is linked to the specific properties of our sample with two distinct transition temperatures T_{C} and T_{MI}.

The tunneling conductance in STS is, for small V and in a simplified picture, proportional to the DOS of both the sample and the tip, to the Fermi function and to the tunneling matrix element, with the latter often described within the Wentzel–Kramers–Brillouin (WKB) approximation. Hence, temperature dependences in STS arise from the Fermi function and—often more importantly—reflect temperature dependences of the sample's DOS. With this, our results for G_0 (figure 2(b)) imply a rapid growth of the DOS right at the Fermi level E_{F} when crossing T_{MI}, reaching a nearly temperature independent low-temperature value as expected for a metal. A similar behavior was observed for $La_{0.6}Pb_{0.43}MnO_3$ single crystals [28] and $La_{0.7}Ca_{0.3}MnO_3$ thin films [16].

In order to provide more direct access to the DOS by minimizing the influence of the tunneling matrix element, the normalized conductance $G_{\mathrm{n}} = (\mathrm{d}I/\mathrm{d}V)/(I/V) = \mathrm{d}(\ln I)/\mathrm{d}(\ln V)$ is generally considered (within certain approximations). The corresponding data for selected temperatures ($T = 30$, 80, 234, 260, 300 K) are presented in figure 4(b). Here, only G_{n} data for $|U - \frac{1}{e}E_{\mathrm{F}}| > 0.1$ V are plotted since G_{n} is ill-defined close to $V = 0$, specifically if a gap-like feature is observed. This implies, however, that the states very close to E_{F} are not visualized even though the strongest changes with temperature are expected in this region. Nonetheless, a significant change of the DOS is obvious as the temperature crosses T_{MI} but, as expected, no effect is observed near T_{C}. For $T < T_{\mathrm{MI}}$, the DOS is strongly energy dependent for both negative and positive bias (i.e. below and above E_{F}) but independent of temperature, the latter in agreement with the argument mentioned above and measurements on single crystals of $La_{0.6}Pb_{0.4}MnO_3$ [28] but in contrast to observations on $La_{0.7}Ca_{0.3}MnO_3$ thin films [16]. The strongly energy-dependent DOS is also reflected in the asymmetry of the $\mathrm{d}I/\mathrm{d}V$ curves at $T < T_{\mathrm{MI}}$, figure 2(b). For $T > T_{\mathrm{MI}}$, the occupied DOS ($V \leqslant 0$) is nearly independent of energy eV. Note that we did not observe a real gap at $V = 0$, rather there is a strong depletion of the DOS close to E_{F} which can be interpreted as a pseudogap [16]. The associated shift of spectral weight might cause the increase of DOS for $T > T_{\mathrm{MI}}$ for $V \lesssim 0$.

In summary, we have observed clear evidence for PS in $Pr_{0.68}Pb_{0.32}MnO_3$ single crystals through spatially resolved STS measurements of the local zero-bias conductance. This PS is restricted to the temperature range between the ferromagnetic and the metal–insulator transition. A drastic change of the DOS close to E_{F} was observed near T_{MI}. It would be interesting—albeit experimentally challenging—to conduct STS in a very close vicinity of T_{MI}.

Acknowledgments

We are grateful to U K Rößler and N D Mathur for valuable discussions. We acknowledge financial support by the European Commission through CoMePhS 517039 and by the DFG through grant WI 1324/1-1.

References

[1] Tokura Y (ed) 2000 *Colossal Magnetoresistive Oxides* (Amsterdam: Gordon and Breach)
[2] Coey J M D, Viret M and von Molnár S 1999 *Adv. Phys.* **48** 167
[3] Millis A J, Littlewood P B and Shraiman B I 1995 *Phys. Rev. Lett.* **74** 5144

[4] Dagotto E 2002 *Nanoscale Phase Separation and Colossal Magnetoresistance* (Heidelberg: Springer)
[5] Moreo A, Yunoki S and Dagotto E 1999 *Science* **283** 2034
[6] Ramakrishnan T V *et al* 2004 *Phys. Rev. Lett.* **92** 157203
[7] Kugel K I *et al* 2005 *Phys. Rev. Lett.* **95** 267210
[8] Uehara M, Mori S, Chen C H and Cheong S-W 1999 *Nature* **399** 560
[9] Zhang L, Israel C, Biswas A, Greene R L and de Lozanne A 2002 *Science* **298** 805
[10] Fäth M *et al* 1999 *Science* **285** 1540
[11] Sarma D D *et al* 2004 *Phys. Rev. Lett.* **93** 097202
[12] Moreo A, Mayr M, Feiguin A, Yunoki S and Dagotto E 2000 *Phys. Rev. Lett.* **84** 5568
[13] Raquet B *et al* 2000 *Phys. Rev. Lett.* **84** 4485
[14] Lu Y *et al* 2006 *Phys. Rev.* B **73** 184406
[15] Moshnyaga V *et al* 2006 *Phys. Rev. Lett.* **97** 107205
[16] Mitra J *et al* 2005 *Phys. Rev.* B **71** 094426
[17] Paranjape M, Raychaudhuri A K, Mathur N D and Blamire M G 2003 *Phys. Rev.* B **67** 214415
[18] Padmanabhan B *et al* 2007 *Phys. Rev.* B **75** 024419
[19] Padmanabhan B 2007 unpublished
[20] Padmanabhan B *et al* 2006 *J. Magn. Magn. Mater.* **307** 288
[21] Li R-W, Zhou X, Shen B-G and Hillebrands B 2005 *Phys. Rev.* B **71** 092407
[22] DeTeresa J M *et al* 1997 *Nature* **386** 256
[23] Rønnow H M, Renner Ch, Aeppli G, Kimura T and Tokura Y 2006 *Nature* **440** 1025
[24] Ma J X, Gillaspie D T, Plummer E W and Shen J 2005 *Phys. Rev. Lett.* **95** 237210
[25] Renner Ch, Aeppli G, Kim B G, Soh Y-A and Cheong S-W 2002 *Nature* **416** 518
[26] Becker T *et al* 2002 *Phys. Rev. Lett.* **89** 237203
[27] Renner Ch and Rønnow H-M 2006 *Scanning Probe Microscopy: Electrical and Electromechanical Phenomena at the Nanoscale* ed S Kalinin and A Gruverman (Berlin: Springer)
[28] Biswas A, Elizabeth S, Raychaudhuri A K and Bhat H L 1999 *Phys. Rev.* B **59** 5368